

# Synthesis and Response of Ku-Band Microwave Characterization of (Bax Ca1-X ZrO3) Ceramic Nanoparticles

Vaishali Mane<sup>1\*</sup>, Shivaji Jadhav<sup>1</sup>, Sarita Shinde<sup>2</sup>

<sup>1</sup>Department of Basic Science and Humanities, Bharati Vidyapeeth Deemed to be University, College of Engineering, Pune-411043, Maharashtra, India.

<sup>2</sup>Department of General Engineering, Bharati Vidyapeeth College of Engineering, Kolhapur-416013, Maharashtra, India.

\*Corresponding Author: Vaishali Mane

Department of Basic Science and Humanities, Bharati Vidyapeeth Deemed to be University, College of Engineering, Pune-411043, Maharashtra, India

Email: [vymane@bvucoep.edu.in](mailto:vymane@bvucoep.edu.in)

## ABSTRACT

The present paper gives a brief insight of preparation of barium calcium zirconate (Bax Ca1-x ZrO3) dense ceramic nano powders by simple solution combustion method. Microwave properties of Barium Calcium Zirconate (Bax Ca1-x ZrO3) investigations are conducted in the Ku-Band (12-18 GHz). Powders were prepared for various compositions of Ba and Ca. X-ray diffraction study was made for studying crystal structure. Scanning electron microscopy (SEM) was employed to analyze the surface morphology of the sintered pellets and to investigate the microstructural features of the samples. With the help of barium calcium zirconate, the structural and morphological properties were investigated as a microwave absorber. With the help of vector network analyser, the microwave properties were calculated. This paper reports compositional variation of Ba and Ca significantly influences the microwave frequency response. For the first time synthesis of barium calcium zirconate (BaCaZrO3) nanoparticles by using a solution combustion process and their characterization in a single-step process was done. This paper reports the dielectric measurements like dielectric constant, loss tangent, and microwave absorption characteristics of the pellets and the sintering behaviour of the nanoparticles in the microwave frequency range.

**Keywords:** Microwave properties, Surface morphology, Vector network analyser.

**How to cite this article:** Mane V, Jadhav S, Shinde S. Synthesis and Response of Ku-Band Microwave Characterization of (Bax Ca1-X ZrO3) Ceramic Nanoparticles. Int J Drug Deliv Technol. 2026;16(59s): 645-652. DOI: 10.25258/ijddt.16.59s.70

**Source of support:** Nil

**Conflict of interest:** None

## Introduction

In the microelectronic world perovskite-type structural dielectric materials have an extraordinary quality for various applications such as displays, sensors, actuators, transducers electronic as well as piezoelectric devices and wireless communications [1]. In recent years, electromagnetic interference (EMI) has emerged as a significant challenge due to the rapid proliferation of electronic devices such as personal computers, personal audio devices, and computer local area networks [2-3]. Electromagnetic pollution at high intensities can significantly disrupt the performance of electronically controlled systems. Moreover, excessive exposure to microwave radiation may pose potential risks to biological systems. To mitigate electromagnetic interference (EMI), the development and application of electromagnetic wave absorbing materials

capable of attenuating unwanted signals are highly recommended. Due to saturation in the sub-gigahertz range, microwaves in the higher gigahertz range are being increasingly utilized in wireless communication, radar and local area network etc. Along with the development of high gigahertz electronics and the trend towards miniature circuits, electromagnetic interference (EMI) is also becoming a serious problem and a matter of crucial concern in higher gigahertz range [4]. In view of that, the mitigation of electromagnetic backscattering through the use of microwave-absorbing materials holds substantial importance in the domain of electromagnetic compatibility. (EMC) [5]. Microwave absorbers have become increasingly important in defence applications, particularly for stealth technology. The application of microwave-absorbing coatings on the external surfaces of military aircraft and vehicles significantly

reduces their radar detectability [6]. Effective microwave absorbing materials require the presence of both electric and magnetic dipoles, which facilitate strong interaction with incident electromagnetic radiation.

The reflection and attenuation characteristics of electromagnetic fields in the radiation are determined by complex permeability and relative permittivity [7-9]. Much research has been done in order to synthesize and characterise an efficient electromagnetic absorber with electromagnetic shielding. Good electromagnetic permeability ( $\mu'$ ) and permittivity ( $\epsilon'$ ) are characterisations of electromagnetic absorber. The real part of permittivity ( $\epsilon'$ ) characterizes the ability of a material to store electric energy when exposed to an electromagnetic field, reflecting its influence on the electric field component. While as, the real part of permeability ( $\mu'$ ) represents the material's capacity to store magnetic energy, indicating its response to the magnetic field component of incident electromagnetic radiation. The electromagnetic wave is attenuated after incidence on certain material; the energy is lost due to dissipation of heat energy. The extent of energy lost depends on the frequency of wave and value of permittivity and permeability of material [10]. Despite over a century of research and development, it has been observed that perovskite material shown that it is essential for applications like as photocatalysis, electrocatalysis, photoelectric conversion, and superconducting technologies [11].

Owing to rapid technological advancements, the microwave region of the electromagnetic spectrum has attracted sustained and significant research interest over the years [12-13]. The solution combustion synthesis (SCS) method is a rapid, energy-efficient and cost-effective technique for the bulk production of nanostructured materials. By using this simple method fabrication of metal oxides are presenting high performance in photocatalytic, energy and environmental applications.

In recent years, microstrip patch antennas offer ample advantages over conservative antenna structures and demonstrate improved performance in many applications. They are

lightweight, low-profile, and easy to fabricate, with the capability to support multiband or multifunctional operation while maintaining compact dimensions and low-profile antenna used as dielectric resonator in the microwave band which has been extensively studied [14-16]. The dielectric materials with moderate dielectric constant, low dielectric loss and high temperature stability have very much importance in packaging technology and communication system [17]. BaZrO<sub>3</sub> and CaZrO<sub>3</sub> are alkaline earth zirconates. These are chemically more stable and stronger in mechanical strength than alkaline earth cerate ceramics [18]. Barium zirconate (BaZrO<sub>3</sub>), with a high melting point of approximately 2700 °C, exhibits excellent high-temperature phase stability, moderate mechanical strength, and low thermal conductivity, thereby making it increasingly significant for applications in the field of electronics [19]. BaZrO<sub>3</sub> replaces Yttria stabilised zirconia (YSZ) which is used as thermal barrier coating for supersonic air jets [20]. Meanwhile, it is also reflected as a promising candidate for high quality crystal growing crucible material for other various high-temperature applications [21-22] the interfacial material for ceramic-ceramic composites [23-24] and substrate for film deposition [25-26].

According to literature survey, Ba ZrO<sub>3</sub> and Ca ZrO<sub>3</sub> has been synthesized, and microwave properties also been studied. But synthesis of Ba Ca ZrO<sub>3</sub> and study of microwave properties was not reported yet. The present study includes synthesis of Barium Calcium zirconate by solution combustion method. The powder was synthesized for various compositions of Ba and Ca. The synthesized powder is sintered at 900°C. Vector network analyser is used to determine the values of  $\epsilon'$ ,  $\epsilon''$ ,  $\mu'$  and  $\mu''$  of barium calcium zirconate at Ku band by using reflection and transmission technique. Barium Calcium Zirconate is fantastic material for microwave absorber. With help of vector network analyser the complex permittivity and permeability as a function of frequency were obtained.

## **Materials and Methods:** **Sample preparation**

In this study all chemical solutions used were of AR grade and procured from LOBA Chemie Company Mumbai. Barium nitrate, glycine, calcium nitrate and zirconium dioxide were purchased from Merck, India. These materials were used as it is received, without any further purification.  $Ba_xCa_{(1-x)}ZrO_3$ , ( $0.1 \leq X \leq 0.5$ ) is synthesised by solution combustion method. The powders of various frequency were different values of x from 0.1 to 0.5 were prepared. The precursors used were  $Ba(NO_3)_2 \cdot 6H_2O$ ,  $Ca(NO_3)_2 \cdot 6H_2O$  and  $ZrO_2$ . The pH value of the precursor solution is 5-8. Glycine is used as fuel. Distilled water from departmental distillation plant was used for the preparation of powders. The precursors in the stoichiometric proportion were used. The powder obtained was of ash colour and turned to fresh white after sintering. Concentrated  $HNO_3$  was added to the aqueous solution containing Ba and Zr ions. The resulting mixture was thoroughly stirred to ensure homogeneous mixing, precipitation or sedimentation. Subsequently, the resulting a perfect solution without any visible precursor was gradually sintered at different temperatures (600°C, 700°C, 800°C, and 900°C) for quite a few hours to obtain crystalline powder. Agate mortar and pestle were used to grind the ash-like product.

X-ray diffraction (XRD) analysis was carried out for the prepared samples to investigate their crystalline structure. The surface morphology of the samples was examined using a scanning electron microscope (SEM). The samples were subsequently sintered, and pellets were fabricated using a hydraulic press under a pressure of 10 tons. Polyvinyl acetate (PVA) was used as a binder during pellet formation. The pellets were prepared with a diameter of 2.2 cm. The microwave properties of the samples were characterized using a vector network analyzer (VNA). Owing to its high dielectric constant and low dielectric loss, barium zirconate ceramics are considered promising materials for a wide range of microwave applications. It is also a widely used for dielectric material and electrically tunable microwave devices.

## Results and discussions

Barium calcium zirconate nano powder was characterized using differential thermal analysis (DTA), thermogravimetric analysis (TGA), and Fourier transform infrared (FTIR) spectroscopy. Figure 1 shows TGA and DTA curve.

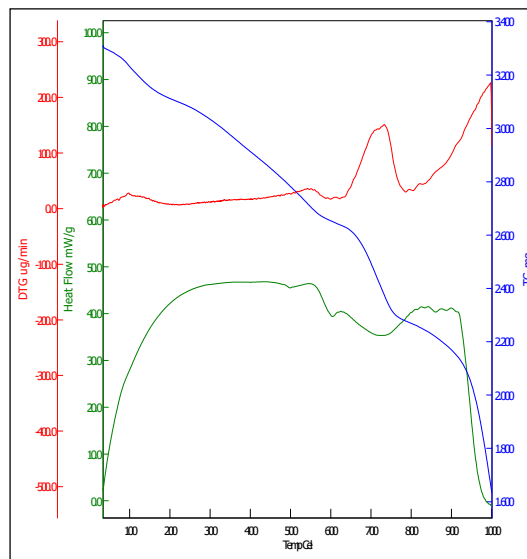


Fig. 1: TGA and DTA curve for  $Ba_xCa_{(1-x)}ZrO_3$ , ( $0.1 \leq X \leq 0.5$ )

TGA and DTA was used to investigate the thermal stability of barium calcium zirconate at heating rate of 2°C in air over a temperature range of 1000°C. TGA curve shows multistep decomposition with no stable intermediary. DTA curve shows that endothermic process takes place at 600°C, which would assign to water removal. The ignition of combustion reaction takes place at 732°C. The exothermic peak is accompanied by mass loss in TGA curve. A noticeable peak around 700–750°C suggests a significant phase changes are occurred. The presence of an exothermic peak in the DTA curve, accompanied by a corresponding mass loss in the TGA profile represents that it is the characteristic of a combustion reaction. The composition and phase structure of the samples were analyzed using X-ray diffraction (XRD).

Figure 2 presents the XRD pattern of  $Ba_xCa_{1-x}ZrO_3$  ( $x = 0.1$ ), which can be well indexed to a cubic perovskite structure. The diffraction peaks at corresponding positions confirm the formation of polycrystalline barium zirconate. The crystallite size was

determined from the value of full width at half maximum (FWHM) of the most intense reflection (101) at 32°, using the Debye Scherrer's formula,

The lattice constant was calculated by using interplaner distance and values of h, k, l planes. The relation used for calculation is,

$$a = \frac{\lambda \sqrt{h^2 + k^2 + l^2}}{2 \sin \theta} \dots \dots \dots (1)$$

Sample	Particle size	Lattice constant (Å)	Volume of unit cell (Å <sup>3</sup> )	Tolerance factor
Ba <sub>x</sub> Ca <sub>(1-x)</sub> ZrO <sub>3</sub>	100nm	6.40	261.144	0.87

$$T = \frac{0.9\lambda}{\beta \cos \theta}$$

where, t is the average diameter in nm. B is the FWHM, λ is the wavelength of X-ray radiation and θ is the Bragg's diffraction angle.

Using XRD, the composition and phase structure of samples were determined. Figure 2 exhibits XRD pattern of Ba<sub>x</sub>Ca<sub>(1-x)</sub>ZrO<sub>3</sub>, (x=0.1) which can be well indexed to the cubic perovskite structure of samples. The peaks at the same locations formed a structure of polycrystalline barium zirconate. The crystallite size was estimated from the full width at half maximum (FWHM) of the most intense (101) diffraction peak at 32°, using the Debye–Scherrer equation.

$$T = \frac{0.9\lambda}{\beta \cos \theta}$$

Using the Scherrer equation, the average crystallite size of Ba<sub>x</sub>Ca<sub>1-x</sub>ZrO<sub>3</sub> was found to be in the range of 20–100 nm. The material exhibits a cubic crystal structure and the corresponding lattice parameter values were a = b = c = 6.40 Å for Ba<sub>x</sub>Ca<sub>(1-x)</sub>ZrO<sub>3</sub> determined accordingly. The c/a ratio was observed to decrease with increasing Ca substitution.

The unit cell volume was calculated by using the relation V=a<sup>3</sup>. The unit cell volume was 264.144 (Å<sup>3</sup>).

Table 1: Sample, particle size (p), lattice constant (a), volume of unit cell (V) and tolerance factor (T)

The perovskite structure of prepared sample was confirmed by calculating tolerance factor (T) by using Goldschmidt relation,

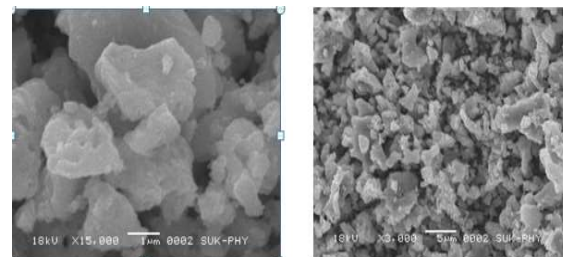
$$T = \frac{R_B + R_O}{\sqrt{2}(R_A + R_O)} \dots \dots \dots (2)$$

The tolerance factor (T) was calculated to be 0.87, confirming the formation of a rhombohedral perovskite structure. X-ray diffraction analysis further reveals that the synthesized powder is single-phase and crystalline in nature, exhibiting a rhombohedral perovskite (ABO<sub>3</sub>) structure with a lattice parameter of a = 6.40 Å.

**SEM characteristics:**

To observe the morphology of samples, SEM images were taken for Ba<sub>x</sub>Ca<sub>(1-x)</sub>ZrO<sub>3</sub> for the compositions of x = 0.1, 0.2, 0.3 and 0.4. SEM was performed on samples of various compositions of Ba and Ca shown in the figure 3. The fundamental morphology is invariant to various contents of Ba and Ca.

**x=0.1**



**x=0.2**

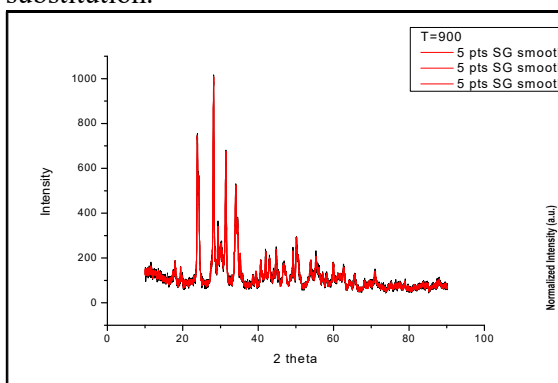
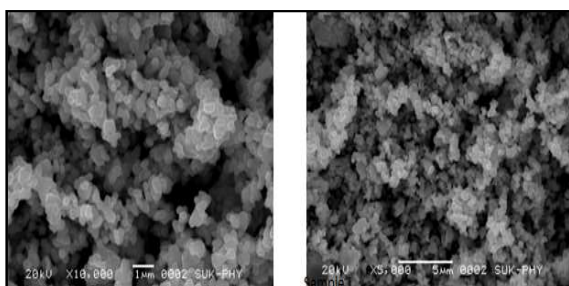
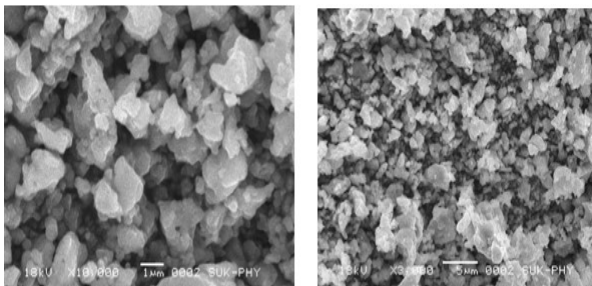


Fig. 2: XRD pattern of Ba<sub>x</sub>Ca<sub>(1-x)</sub>ZrO<sub>3</sub>, (x=0.1)



x=0.3



x=0.4

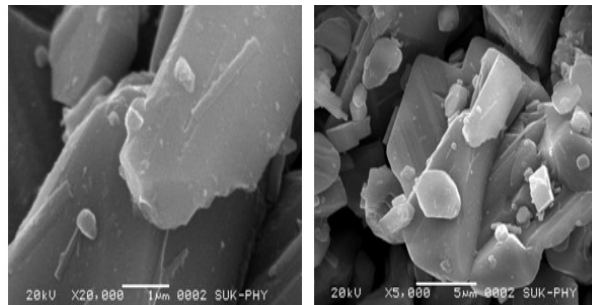


Fig. 3. SEM micrographs of  $Ba_x Ca_{(1-x)} ZrO_3$  for the compositions of  $x = 0.1, 0.2, 0.3$  and  $0.4$

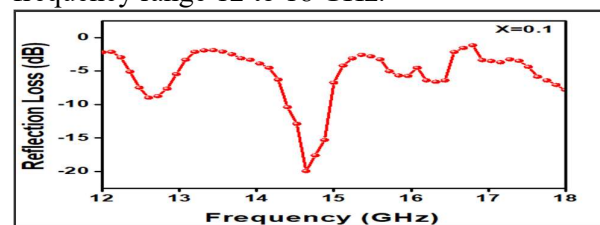
The microstructures of the synthesized powders display consistent and homogeneous morphological patterns. SEM micrographs of  $Ba_x Ca_{(1-x)} ZrO_3$  the material exhibits a polycrystalline and agglomerated morphology. The primary particles are formed by randomly oriented grains. These particles assemble to larger, dense microstructures with a high number of aggregates and a small number of micro pores.

**Microwave properties:** The microwave dielectric constants of sintered pellets were found to be decreased from 36.40 to 20.03 and the value of  $\tau_f$  changed from 364.63 to 54.63 ppm/ $^{\circ}C$ .

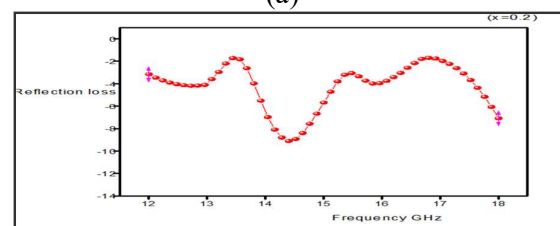
Figure 4 (a, b, c, d and e) presents the experimentally obtained reflection loss as a function of frequency for various Ba and Ca compositions, measured using a vector network analyzer. The composition

parameter  $x$  varies from 0.1 to 0.5, as illustrated in the figure.

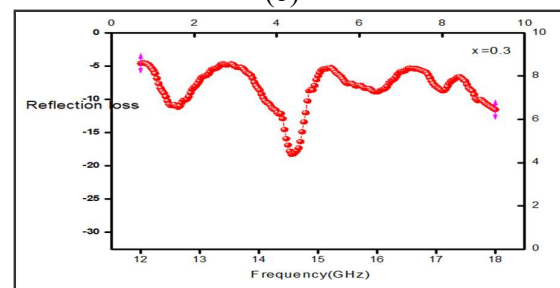
All samples of barium calcium zirconate showed good microwave absorption. Table 2 depicts the reflection loss (RL) values of  $Ba_x Ca_{(1-x)} ZrO_3$  with the different compositions. For the value of  $x=0.1$ , the  $R_l$  value was -22dB. For  $x=0.2$ , the  $R_l$  value was -9dB. For  $x=0.3$ , the  $R_l$  value increases to -20dB and for  $x=0.5$ , it reached to -29dB.  $R_l$  value showed random variation with compositions. All the variations were studied in the microwave frequency range 12 to 18 GHz.



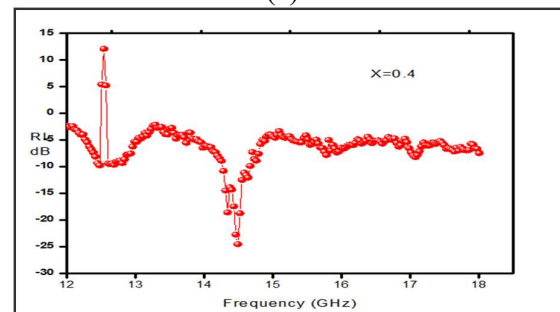
(a)



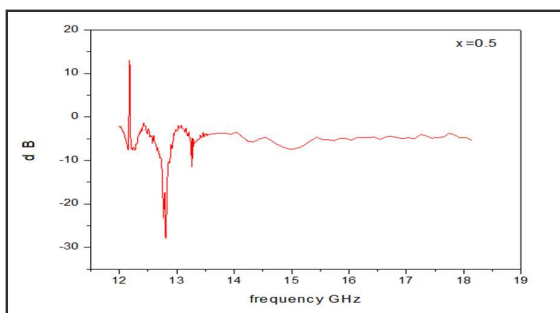
(b)



(c)



(d)



(e)

Fig. 4. The reflection loss (RL) of  $\text{Ba}_x \text{Ca}_{(1-x)} \text{ZrO}_3$  sample ( $x = 0.1-0.5$ ) in the frequency range of 12 to 18 GHz

Figure 4 shown that the reflection loss analysis of  $\text{Ba}_x \text{Ca}_{1-x} \text{ZrO}_3$  samples ( $x = 0.1-0.5$ ) reveals strong composition-dependent and frequency-dependent microwave absorption behavior in the Ku-band (12–18 GHz). Among all compositions, the samples with  $x = 0.4$  and  $x = 0.5$  exhibit superior absorption performance, achieving maximum reflection loss values of approximately  $-25$  dB and  $-30$  dB, respectively, indicating excellent attenuation capability. The absorption peaks are observed to shift with variation in composition, demonstrating tunable microwave absorption characteristics. The enhanced performance at higher  $x$  values can be attributed to improved impedance matching and increased dielectric loss mechanisms. Additionally, the presence of multiple absorption bands across the frequency range suggests effective broadband absorption behavior.

Table 2. The reflection loss (RL) values of  $\text{Ba}_x \text{Ca}_{(1-x)} \text{ZrO}_3$  with the different compositions

Composition	Maximum value of RI (Reflection loss) (dB)	Frequency (GHz)
0.1	-22	14.6
0.2	-9	14.5
0.3	-20	14.8
0.4	-25	14.6
0.5	-29	12.9

### Conclusion

Ceramic materials are known for their chemical stability and high temperature resistance. Barium Calcium Zirconate ( $\text{Ba}_x \text{Ca}_{(1-x)} \text{ZrO}_3$ ) is a promising perovskite oxide ceramic material for microwave absorber applications. Ceramic materials are known for their chemical stability

and high temperature resistance. The substitution of calcium into the barium zirconate lattice significantly modifies the dielectric properties and enhances microwave absorption performance. SEM images show porous natures of powder. Nano size particles were obtained. The perovskite structure provides excellent thermal stability, structural integrity, and dielectric polarization mechanisms that contribute to effective microwave energy dissipation. The study demonstrates that  $\text{Ba}_x \text{Ca}_{(1-x)} \text{ZrO}_3$  exhibits suitable dielectric constant and loss characteristics required for microwave absorbing materials. Owing to its high dielectric constant and low dielectric loss, nanocrystalline  $\text{Ba}_x \text{Ca}_{1-x} \text{ZrO}_3$  emerges as a promising material for microwave absorption and electromagnetic interference (EMI) shielding applications, particularly in microwave communication and radar systems. The results further confirm that Ca-substituted barium zirconate in nanocrystalline form is a potential candidate for advanced microwave absorption and electromagnetic applications. Overall, the synthesized materials exhibit significant potential as efficient microwave absorbing materials for electromagnetic interference (EMI) shielding and radar absorbing applications, particularly in the Ku-band region.

**Conflict of Interest:** There is no conflict of interest.

### References

1. K. Uchino, *Ceramic International*, **21**, 309, (1995); [https://doi.org/10.1016/0272-8842\(95\)96202-Z](https://doi.org/10.1016/0272-8842(95)96202-Z).
2. K. M. Lim, M. C. Kim, K.A. Lee and C.G Park, *IEEE Transactions on Magnetics*, **39**, 1836, (2003); <https://doi.org/10.2528/PIERM12072303>
3. Santoshi Sugimoto, Katsumi Okayama, Sin-Ichi Kondo and Motofumi Homma, *Material Transactions JIM*, **39**, 1080, (1998); <https://doi.org/10.1109/20.801112>
4. Tatiana Giannakopoulou, Apostolos Kontogeorgakos and George Kordas,

- Journal of Magnetism and Magnetic materials*, **263**, 173, (2003);  
[https://doi.org/10.1016/S0304-8853\(02\)01551-2](https://doi.org/10.1016/S0304-8853(02)01551-2)
5. Parveen Singh, V. K. Babbar, Archana Razdan, R. K. Puri and T. C. Goel, *Journal of Applied Physics*, **87**, 4362, (2000);  
<https://doi.org/10.1063/1.373079>
  6. Dieter Janke, *Metallurgical Transactions B*, **13**, 227, (1982);  
<https://doi.org/10.1007/BF02664579>
  7. P. Saini, V. Choudhary, B.P. Singh, Mathur and S.K. Dhawan, *Materials Chemistry and Physics*, **113**, 919, (2009);  
<https://doi.org/10.1016/j.matchemphys.2008.08.065>
  8. L. E. Cross and T. R. Gumraja, *MRS online proceedings library*, **72**, 53, (1986);
  9. K. Wakino, *Proceedings of the 6th IEEE International Symposium on Applications of Ferroelectrics*, (Bethlehem, PA (IEEE, Piscataway NJ), 97, (1986);
  10. R. Vassen, X.Q. Cao, F. Tietz, D. Basu, and D. Stoeber, *Journal of American Ceramic Society.*, **83**, 2023, (2000);  
<https://doi.org/10.1111/j.1151-2916.2000.tb01506.x>
  11. Dmitry Medvedev, Julia Lyagaeva, E.V. Gorbova, A.K. Demin and Panagiotis Tsiakaras, *Progress in Material Science.*, **7**, 38, (2016);  
<https://doi.org/10.1016/j.pmatsci.2015.08.001>
  12. S. Parida, S.K. Rout, L.S. Cavalcante, E. Sinha, Li M. Siu, V. Subramanian, N. Gupta, V.R. Gupta, J.A. Varela and E. Longo, *Ceramics International*, **38**, 2129, (2012);  
<https://doi.org/10.1016/j.ceramint.2011.10.054>
  13. Y.C. Lee, K.W. Weng, W.H. Lee., and Y.L. Huang, *Journal of the Ceramic Society of Japan*, **117**, 1363, (2009); <https://doi.org/10.2109/jcersj2.117.402>
  14. C. Edward, Niehenke, A. Robert, Pucel, Inder J. Bahl, *IEEE Transactions Microwave Theory & Techniques*, **50**, 846, (2002);  
<https://doi.org/10.1109/22.989968>
  15. Ying-Chieh Lee, Ko-Wei Weng, Wen-Hsi Lee, Yen-Lin Huang, *Journal of Ceramic Society of Japan*, **117**, 402, (2009);  
<https://doi.org/10.2109/jcersj2.117.402>
  16. U. Kaatz, *Metrologia*, **47**, 91, (2010);  
<https://doi.org/10.1088/0026-1394/47/2/006>
  17. Koji Katahira, Yoshirou Kohchi, Tetsuo Shimura, H. Iwahara, *Solid State Ionics*, **138**, 91, (2000);  
[https://doi.org/10.1016/S0167-2738\(00\)00777-3](https://doi.org/10.1016/S0167-2738(00)00777-3)
  18. Hans G. Bohn and T. Schober, *Journal of American Ceramic Society*, **83**, 768, (2004); <https://doi.org/10.1111/j.1151-2916.2000.tb01272.x>.
  19. Yuchen Liu, Wei Zhang, Banghui Wang, Luchao Sun, Fangzhi Li, Zhenhai Xue, Bin Liu, N. Hongqiang, *Ceramic International*, **44**, 16475, (2018);  
<https://doi.org/10.1016/j.ceramint.2018.06.064>
  20. Zhe Qiao, Yuanbing Li and Jianing Wang, *Ceramics International*, **47**, 31194, (2021);  
<https://doi.org/10.1016/j.ceramint.2021.07.295>
  21. R. Terki, G. Bertrand and H. Aourag, *Microelectronic Engineering*, **81**, 514, (2005);  
<https://doi.org/10.1016/j.mee.2005.04.004>
  22. Plummer, John, *Nature Materials*, **15**, 819, (2016); <https://doi.org/10.1038/nmat4699>.
  23. Nitin P. Pature, *Nature Materials*, **15**, 804, (2016);  
<https://doi.org/10.1038/nmat4687>
  24. Robert Vassen, Xueqiang Cao, Frank Tietz, Debabrata Basu and Detlev Stover, *Journal of the American Ceramic Society*, **83**, 2023, (2004);  
<https://doi.org/10.1021/acsami.3c16681a>

25. David R. Clarke, Matthias Oechsner, and Nitin P. Padture, *MRS Bulletin*, **37**, 891, (2012); <https://doi.org/10.1557/mrs.2012.238>
26. Gregoire Witz, Markus Schaudinn, Joerg Sopka and Tobias Buecklers, *Journal of Eng. Gas turbines Power-conference: ASME Turbo Expo*, **7,1** (2016); <https://doi.org/10.1115/GT2016-57425>